Measurements of long-range correlations in photonuclear collisions with ATLAS

Blair Daniel Seidlitz
University of Colorado Boulder
for the ATLAS collaboration

Initial Stages 2021, Jan. 11th

Which small systems do we know flow?

pp

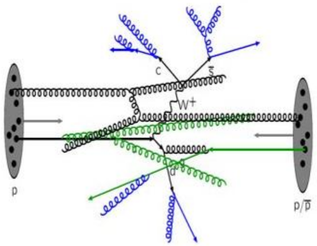

Near-side ridge

Which small systems do we know flow?

pp	e+*p*	e^++e^-	γ+*p*
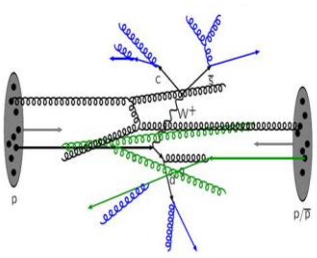	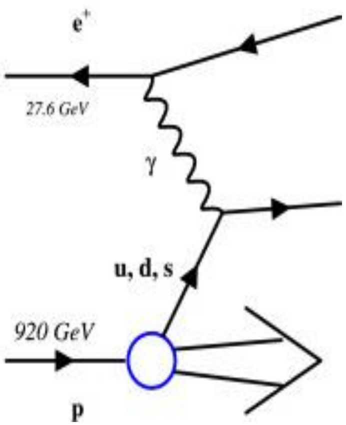	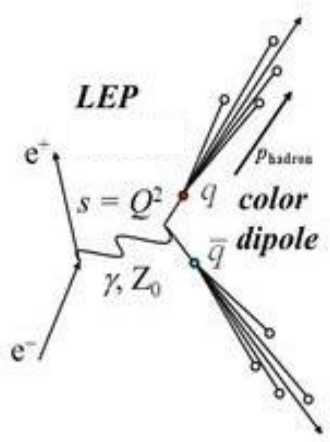	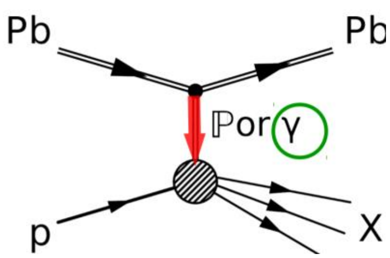
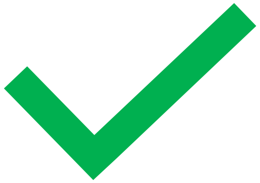			
Near-side ridge	Cumulants say v_2< 5%	No near-side ridge	No near-side ridge
	arXiv:1912.07431	arXiv:1906.00489	CMS-PAS-HIN-18-008

Which small systems do we know flow?

pp

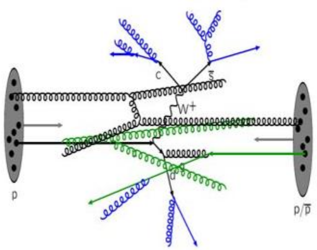

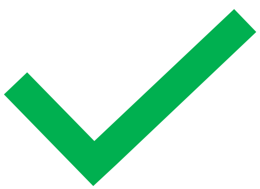

Near-side ridge

e+*p*

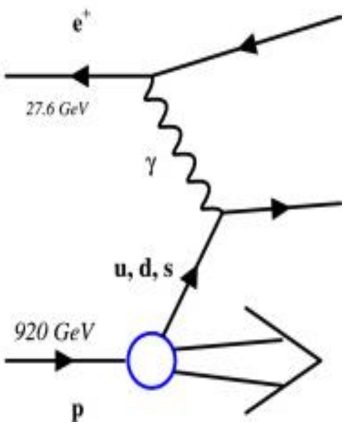

Cumulants
say $v_2 < 5\%$

arXiv:1912.07431

$e^+ + e^-$

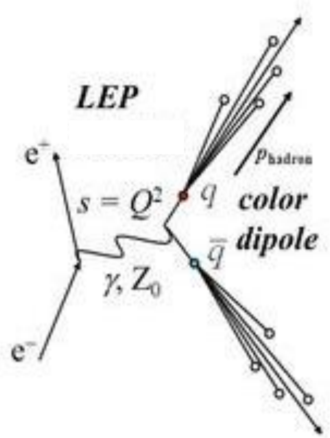

No
near-side ridge

arXiv:1906.00489

γ+*p*

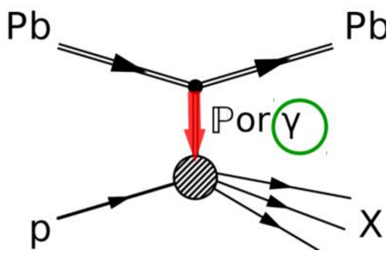

No
near-side ridge

CMS-PAS-HIN-18-008

γ+A

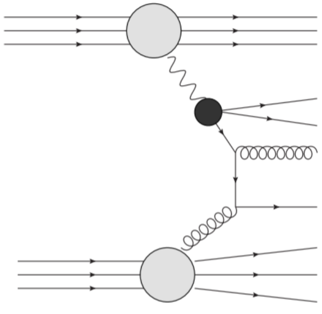

Ultra-peripheral collisions with ATLAS

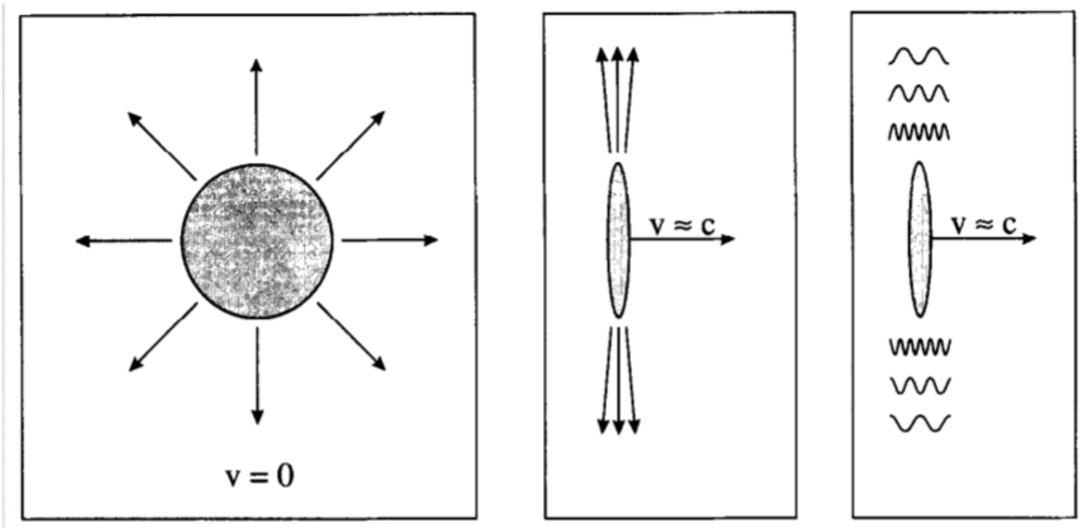

Coulomb fields of moving charges can be treated as an equivalent flux of photons which are boosted to high energies.

Photons reach energies of 10s of GeV with 5.02 TeV Pb+Pb at the LHC

When $b > 2R_A$ two categories of interactions

- Pure EM processes
  - $\gamma\gamma \rightarrow \gamma\gamma$ arXiv:1904.03536 & arXiv:2008.05355 **NEW**
  - $\gamma\gamma \rightarrow \mu\mu$ arXiv:2011.12211 **NEW**
- Photonuclear interactions
  - $\gamma + A \rightarrow A^* + V$
  - $\gamma + A \rightarrow X$

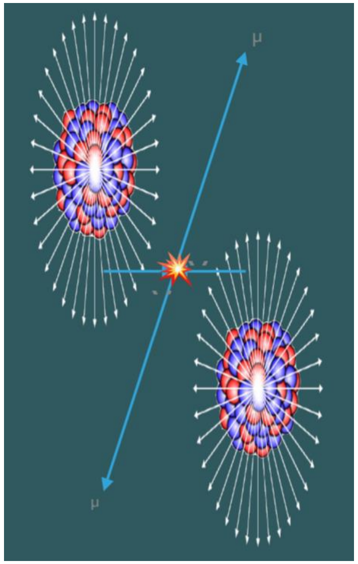

Photonuclear interactions

Direct γA collisions

Photon couples directly to nuclear parton

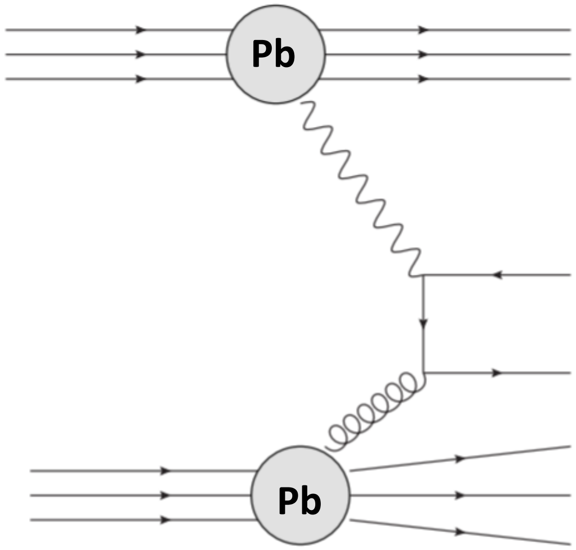

Photonuclear interactions

Direct γA collisions

Photon couples directly to nuclear parton

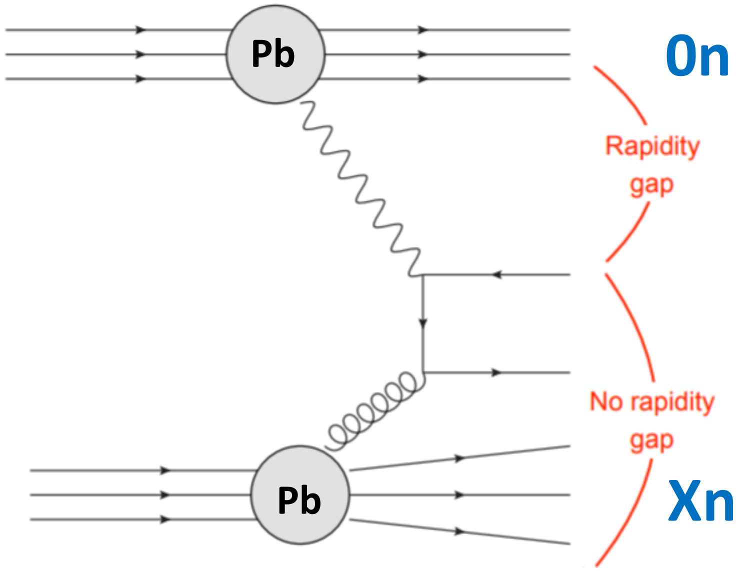

Photonuclear interactions

Direct γA collisions

Photon couples directly to nuclear parton

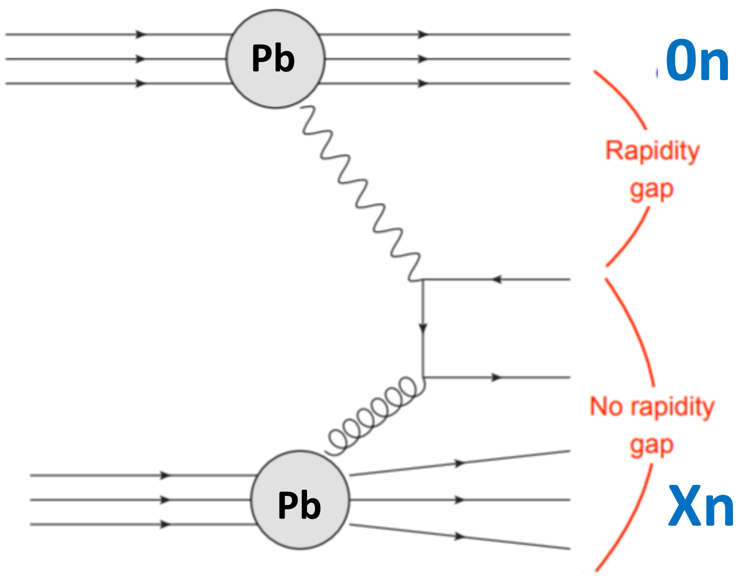

Resolved γA collisions

photon virtually resolved into <u>hadronic state</u>

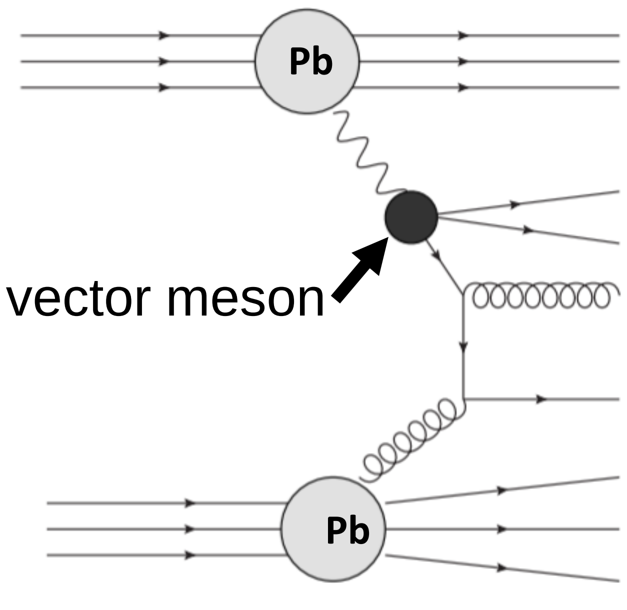

Photonuclear interactions

Direct γA collisions

Photon couples directly to nuclear parton

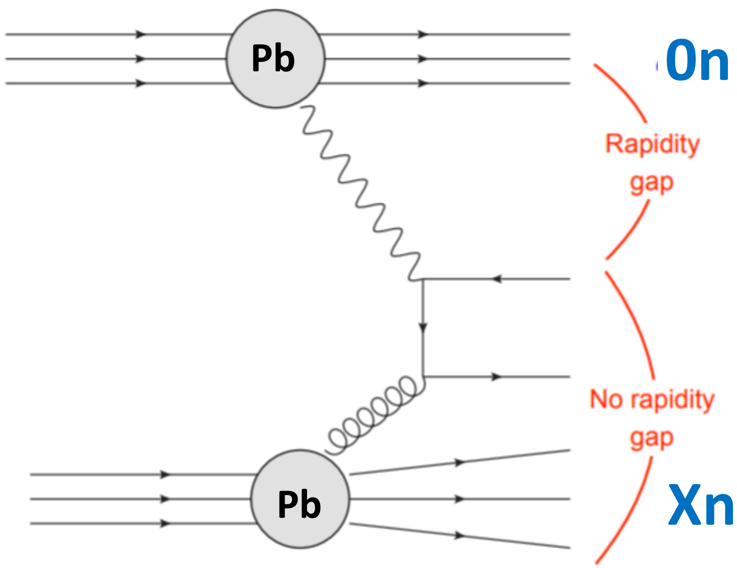

Resolved γA collisions

photon virtually resolved into hadronic state

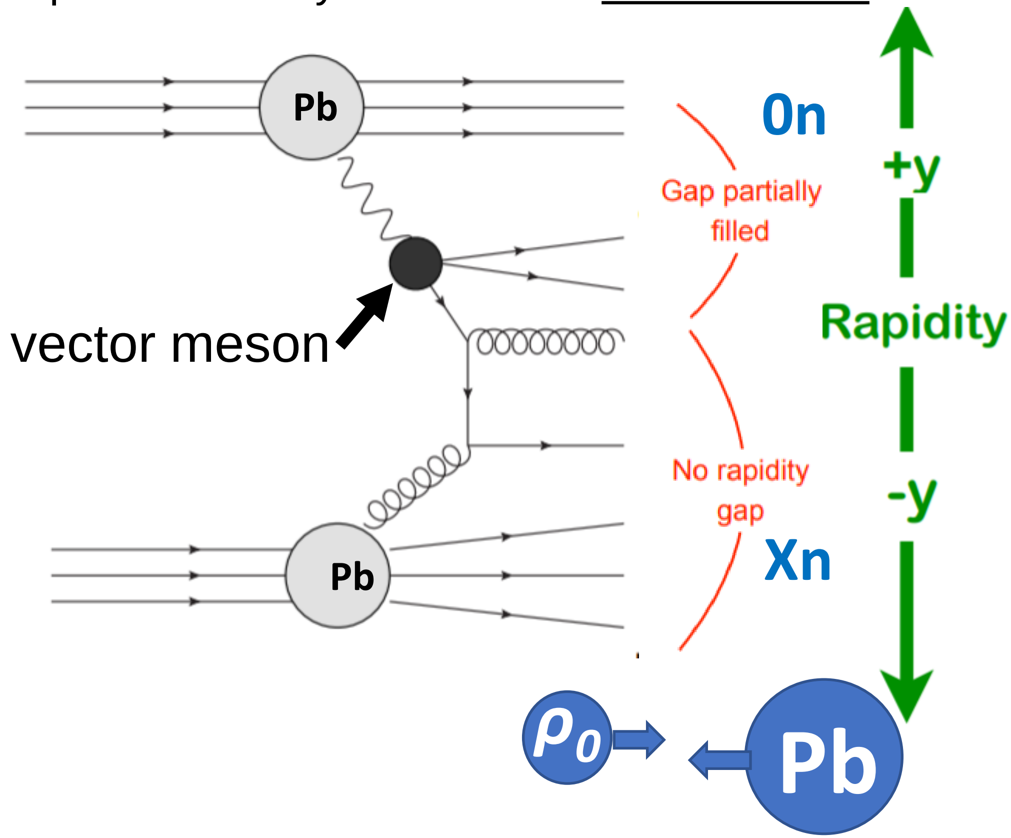

Select events based on primarily

- Single-sided nuclear breakup “**0nXn**” (zero-degree calorimeter ZDC)
- Rapidity gaps

Minimum bias selection includes both but is dominated by resolved events.

"High"-multiplicity photonuclear collisions

Pb going direction

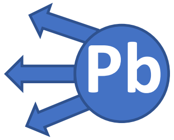

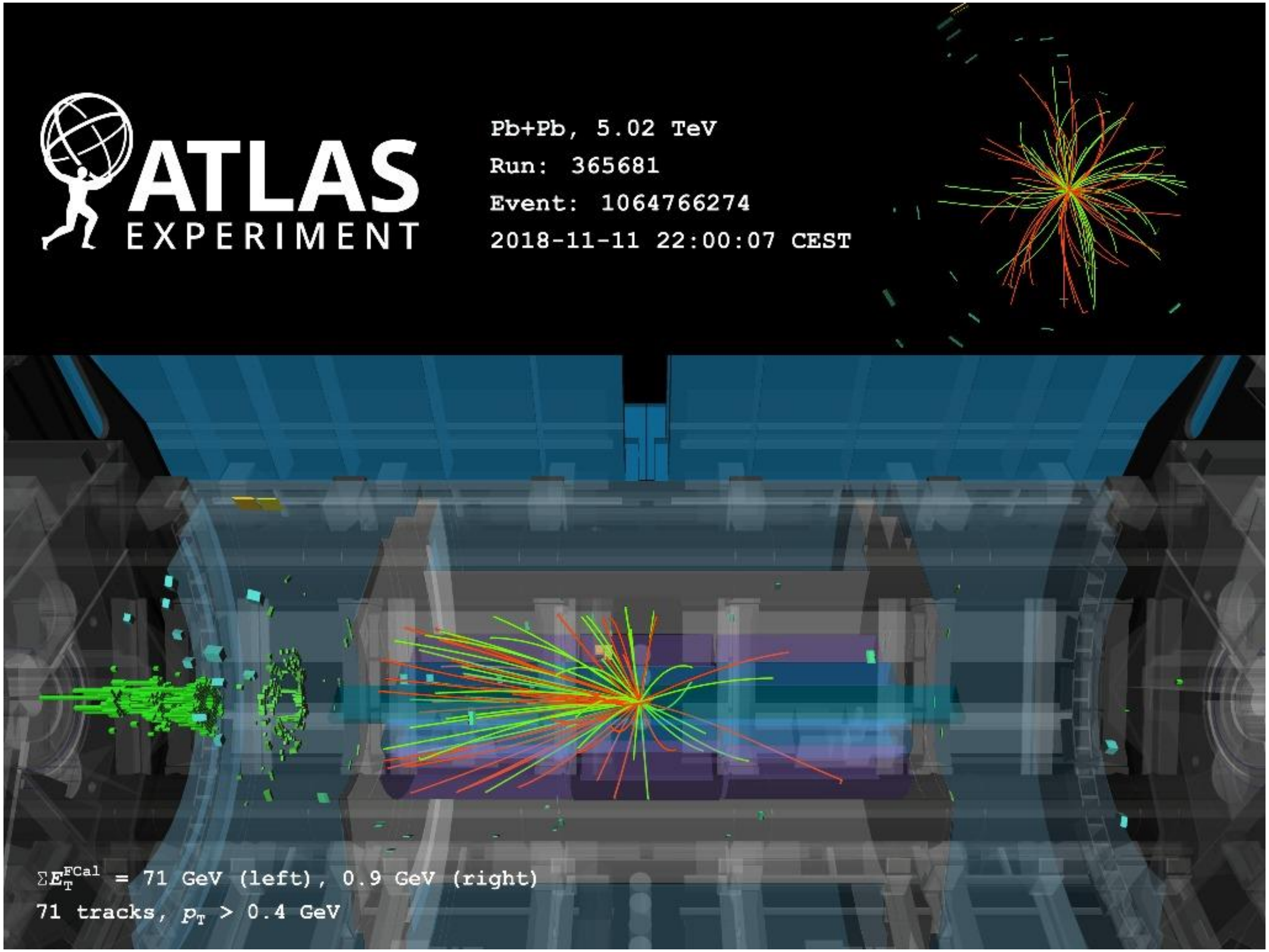

photon going direction

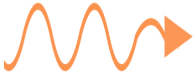

“High”-multiplicity photonuclear collisions

Pb going direction

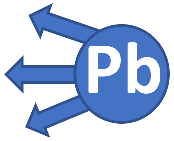

Xn

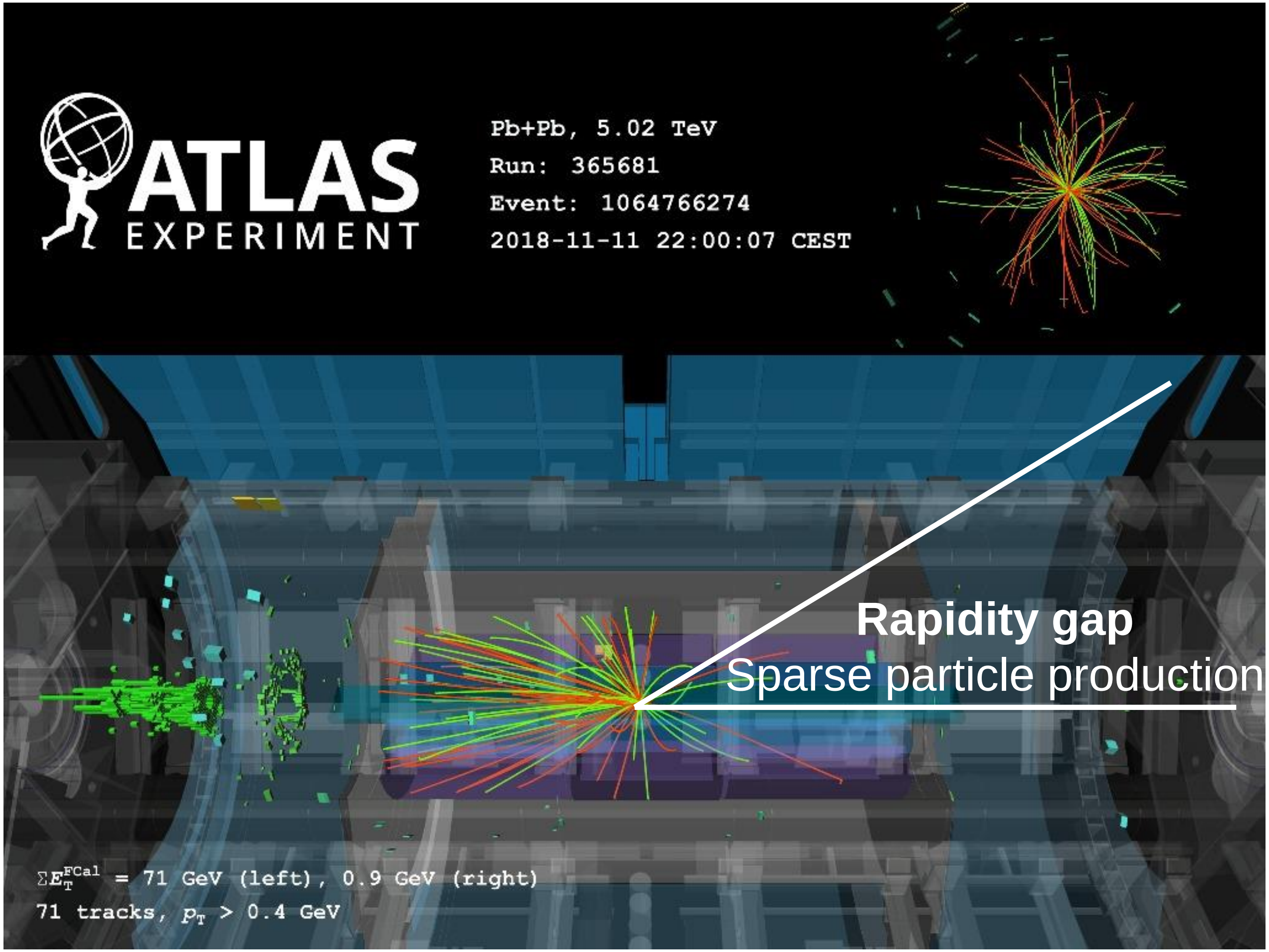

photon going direction

0n

Photonuclear rapidity gaps $\Sigma_\gamma\Delta\eta$ and N_{ch}

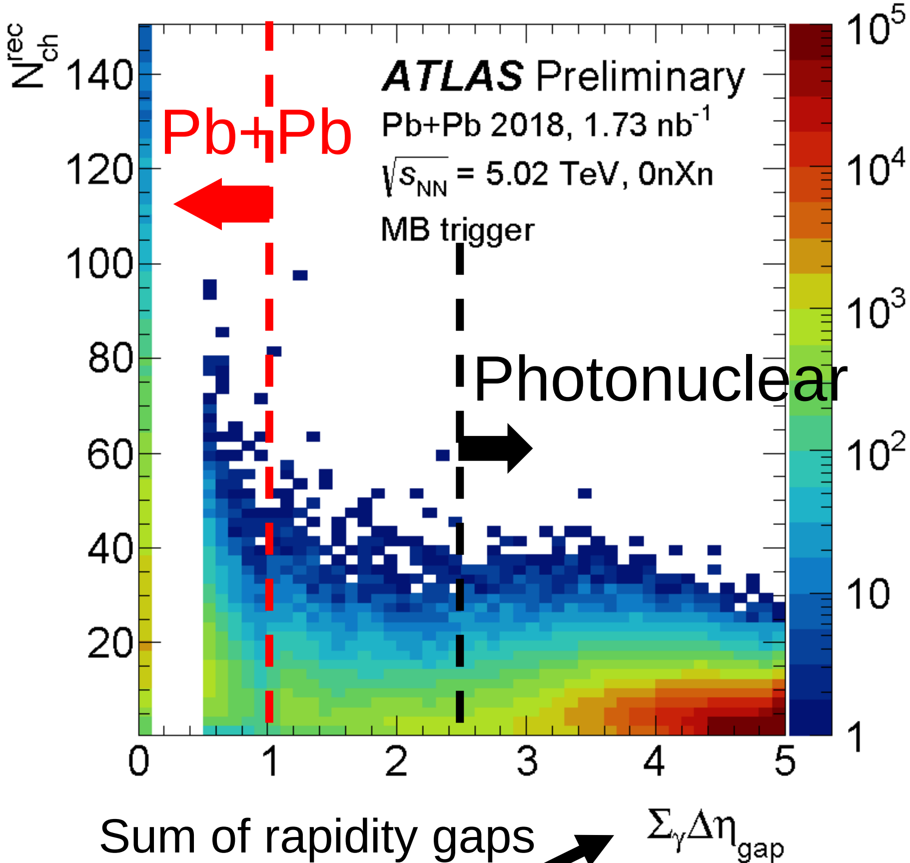

Sum of rapidity gaps between particles greater than 0.5

Photonuclear rapidity gaps $\Sigma_\gamma \Delta\eta$ and N_{ch}

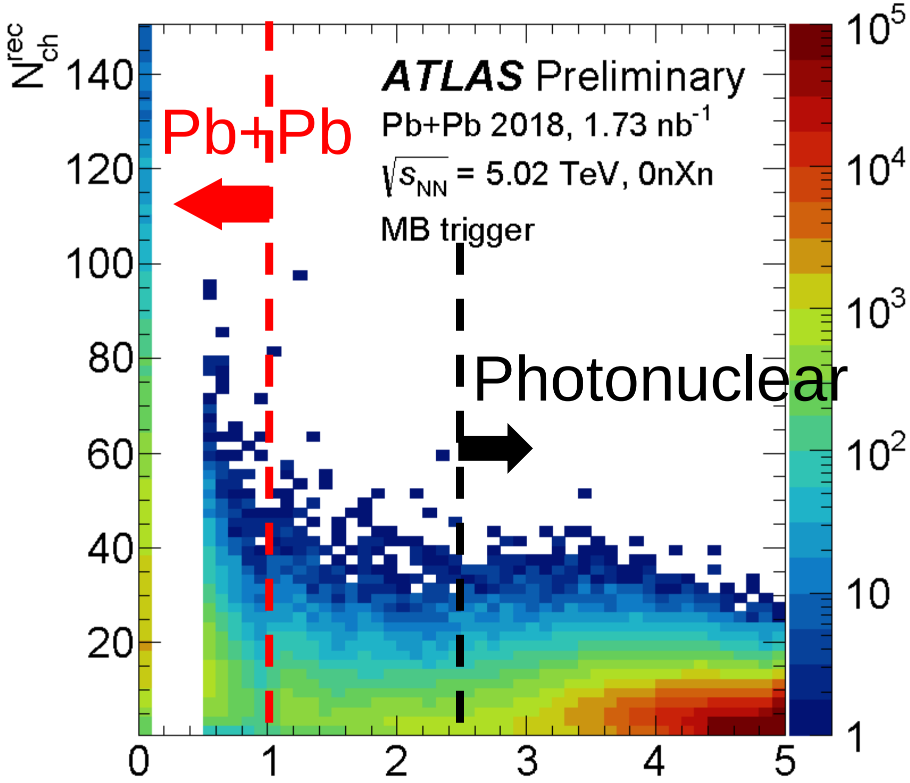

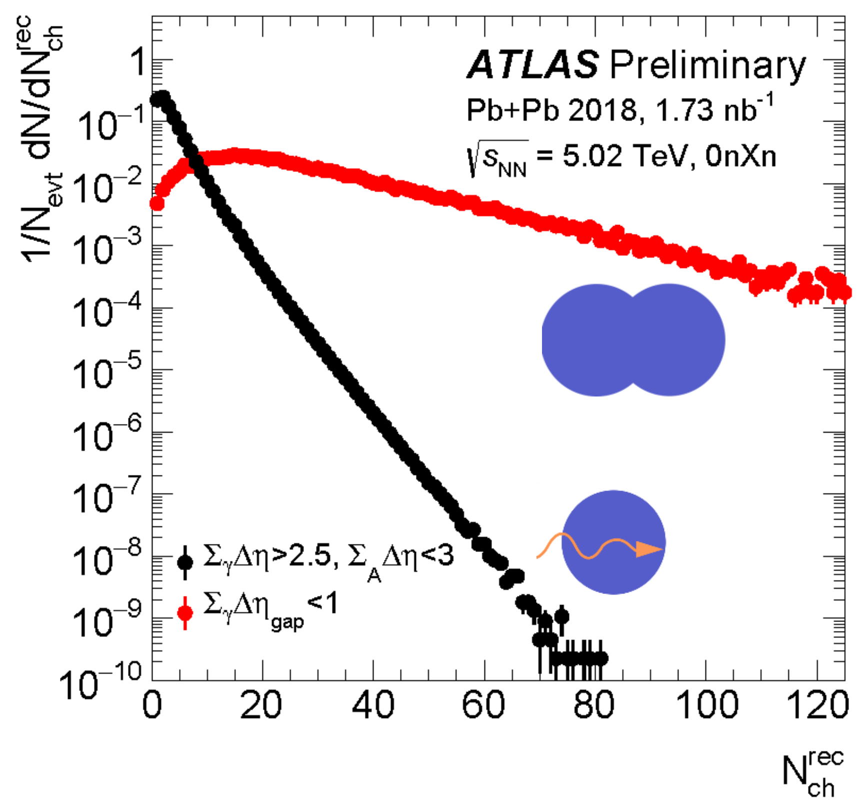

Sum of rapidity gaps between particles greater than 0.5

$|\eta|<2.5$, $p_T>400$ MeV

Photonuclear events have large rapidity gaps in the photon-going direction and a steeply falling multiplicity distribution.

ATLAS-CONF-2019-022

Photonuclear event properties

Several data-MC comparisons included in our new results!

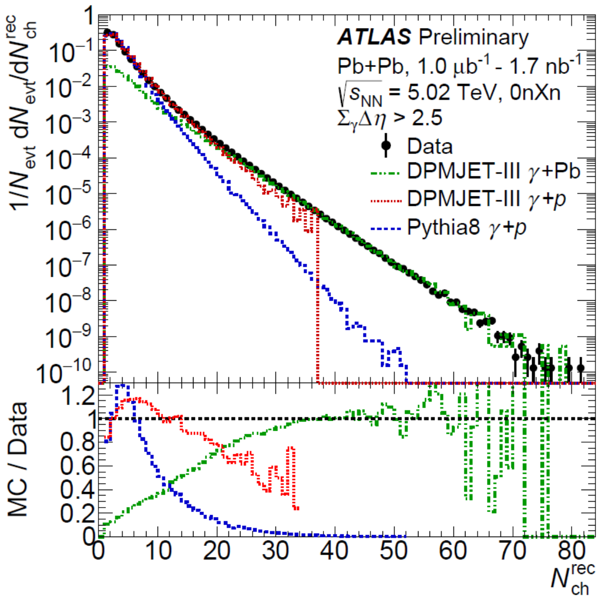

N_{ch}

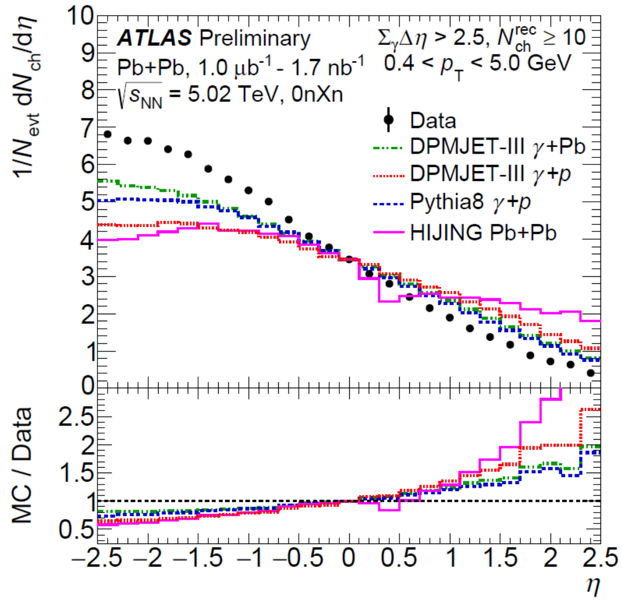

$dN_{ch}/d\eta$

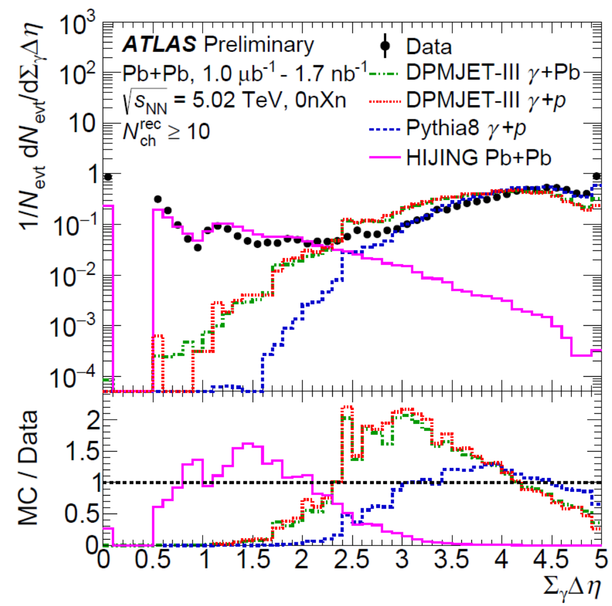

$\Sigma_\gamma \Delta\eta$

CERN-EP-2020-246

Photonuclear event properties

Several data-MC comp

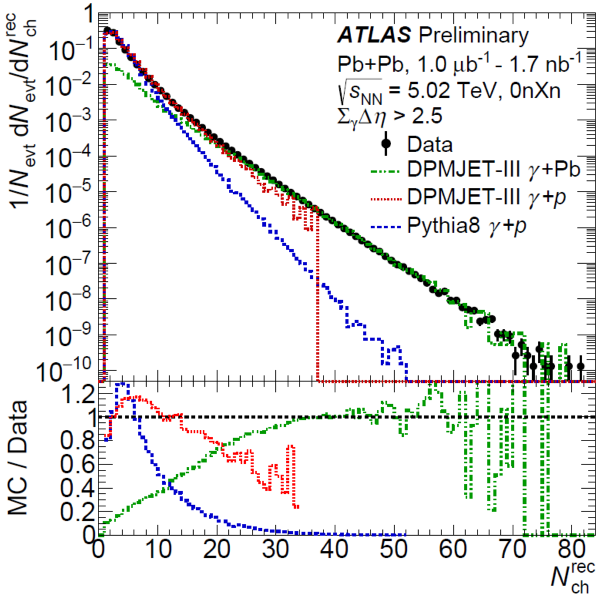

***N*ch**

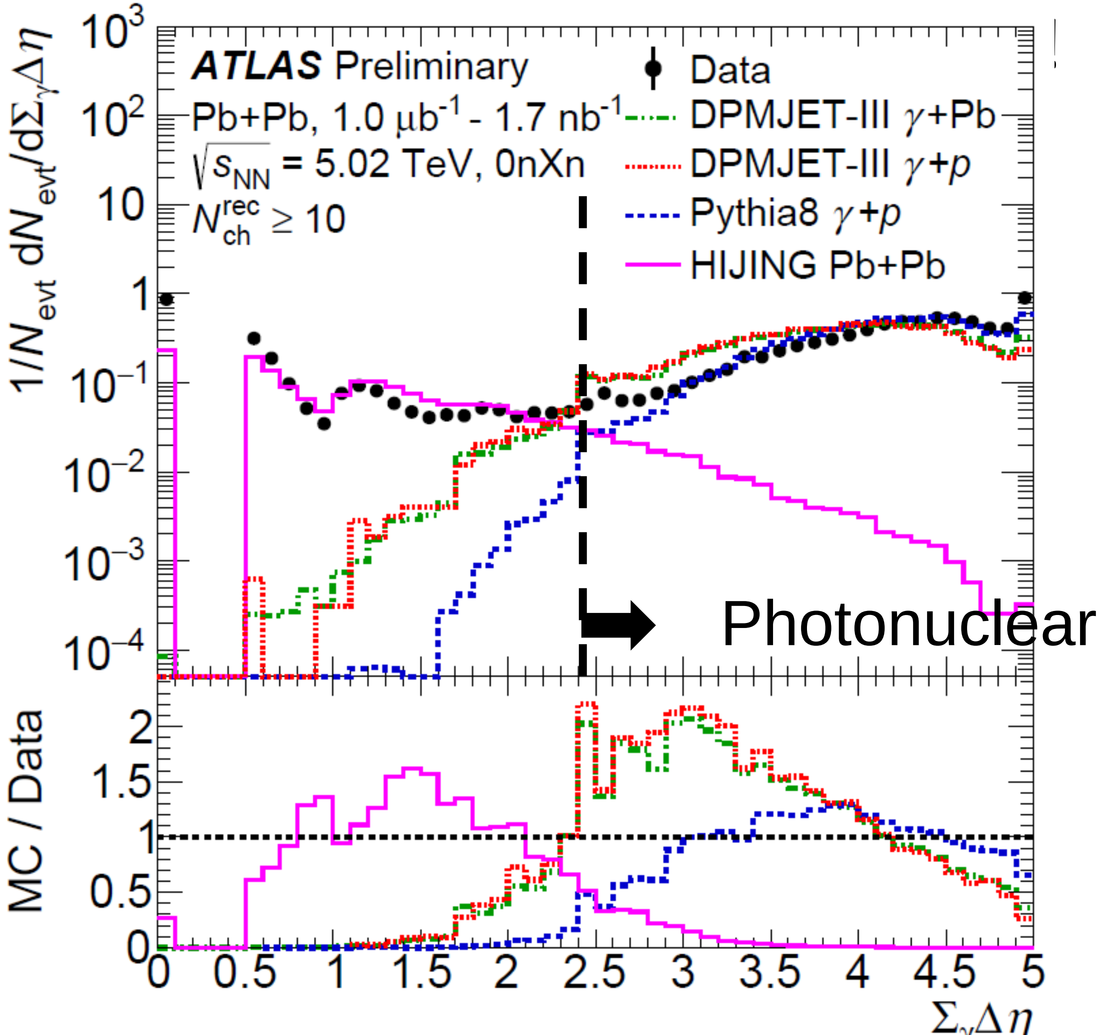

CERN-EP-2020-246

> 97% purity across N_{ch} range of analysis

ATLAS template fit to γA correlation

High-multiplicity (HM) correlation data

Low multiplicity (LM) template for jet/nonflow correlation

$$Y^{\mathrm{HM}}(\Delta\phi) = FY^{\mathrm{LM}}(\Delta\phi) + G\left\{1 + 2\sum_{n=2}^{3} v_{n,n}\cos(n\Delta\phi)\right\}$$

HM – (scaled LM) removes nonflow

Clear **cos(2Δϕ)** modulation

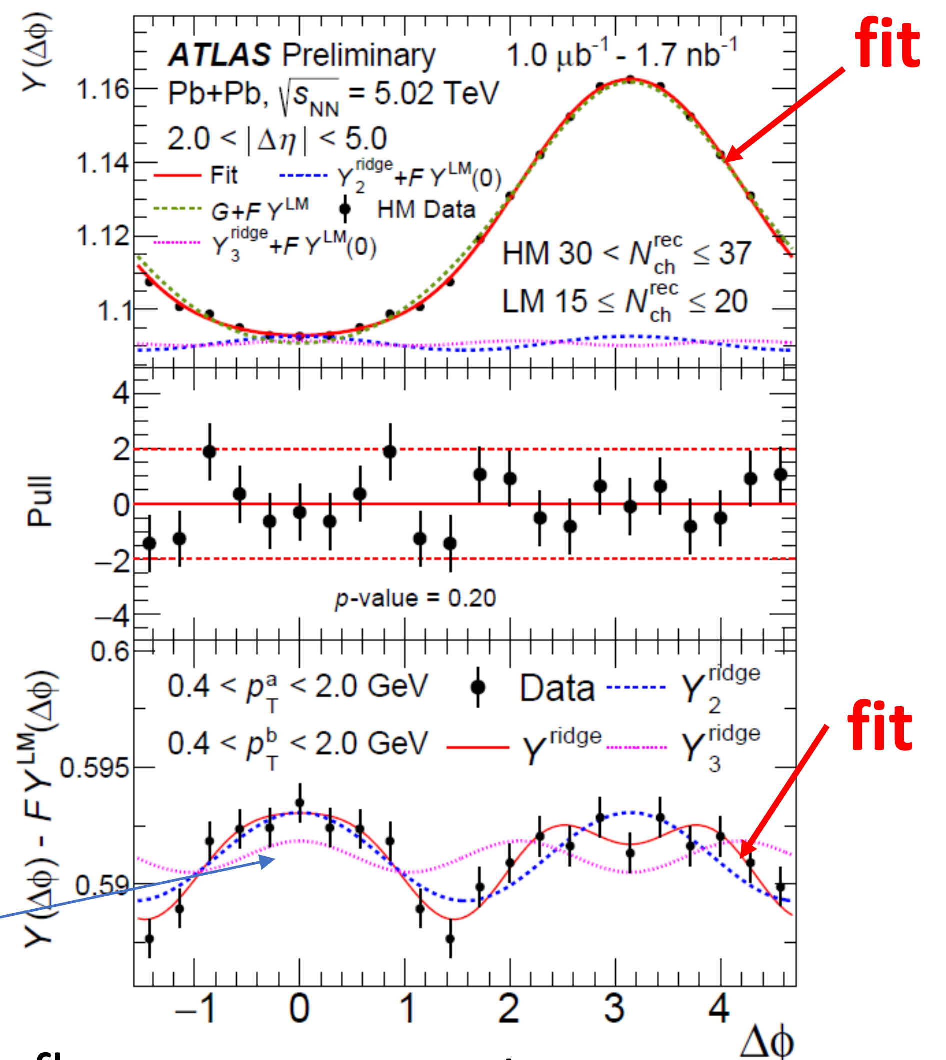

Same technique used in *pp* and *p*+Pb flow measurements

CERN-EP-2020-246

v_n in photonuclear collisions

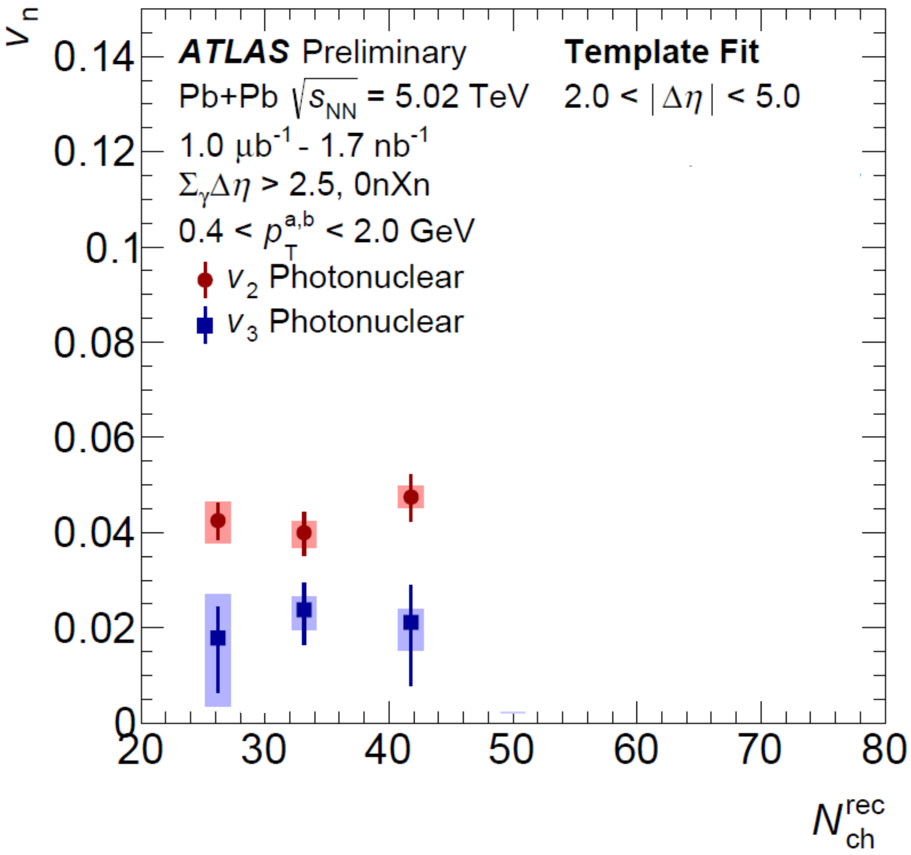

Significant nonzero v_2 and v_3 in photonuclear collisions

Flat $v_2(N_{ch})$ within statistical precision

CERN-EP-2020-246

v_n in photonuclear collisions

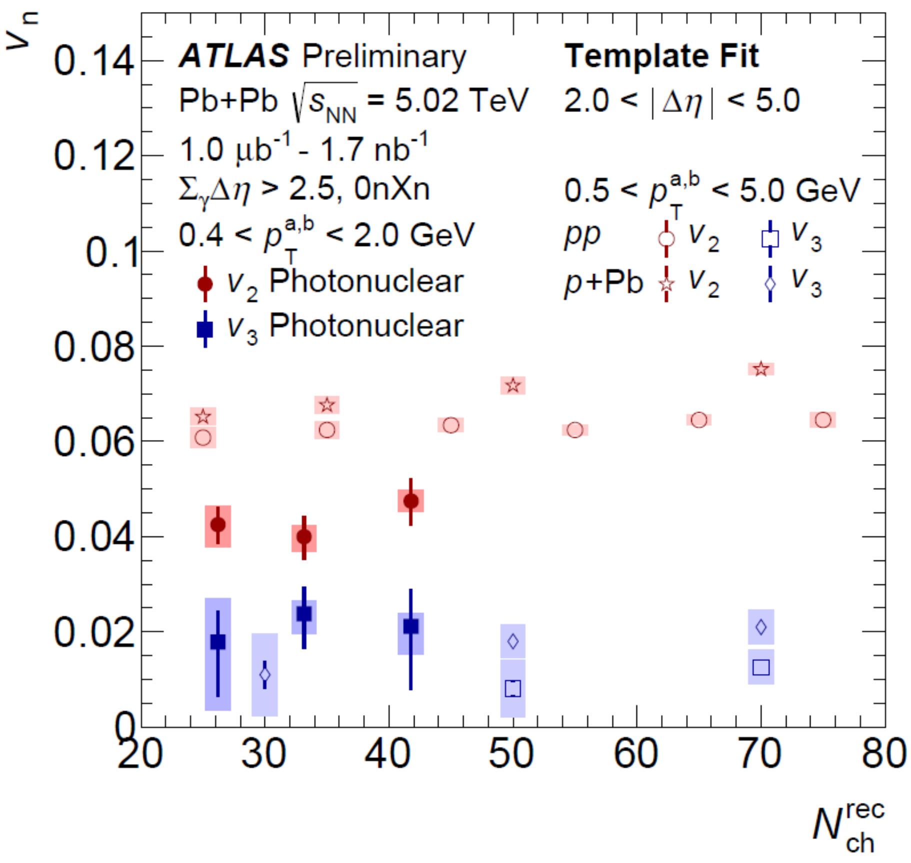

Significant nonzero v_2 and v_3 in photonuclear collisions

Flat $v_2(N_{ch})$ within statistical precision

Changing *pp* to 0.4 < p_T < 2.0 is predicted to lower *pp* v_2 by ~10% which does not lead to agreement between *pp* and γA

Consistent v_3 between γA and *pp* given large uncertainties on both

CERN-EP-2020-246

$v_2(p_T)$ comparison with *pp* and *p*+Pb

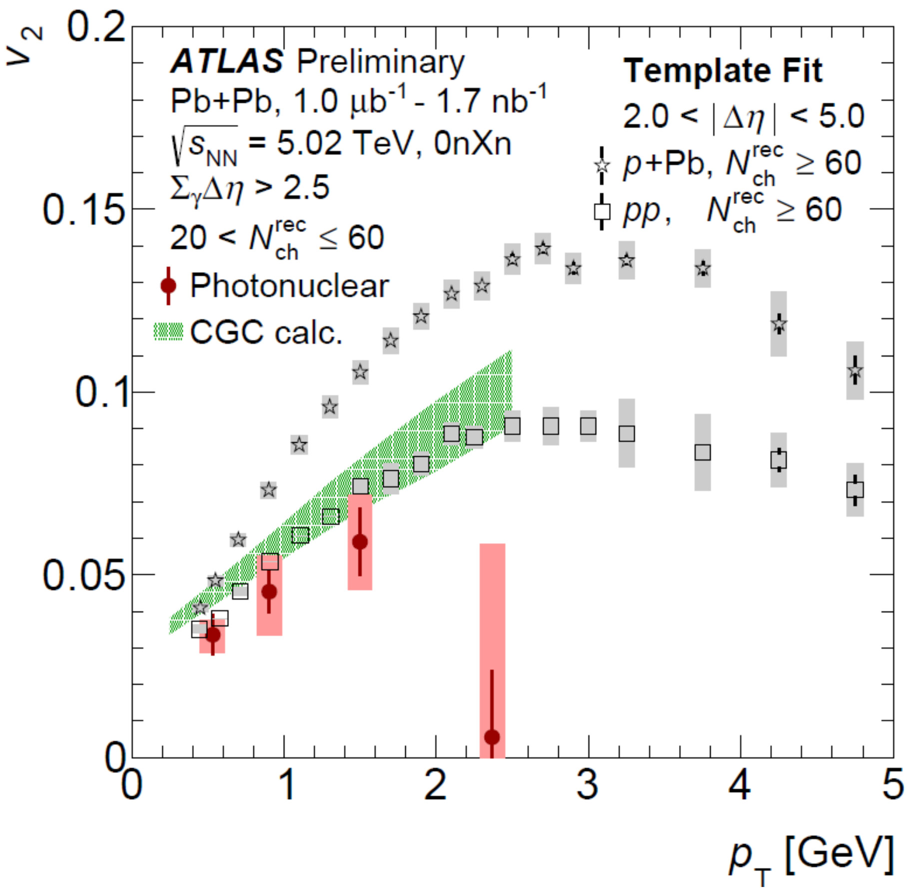

CERN-EP-2020-246

Similar trend in $v_2(p_T)$ as other hadronic systems.

Similar low-p_T behavior as *pp* and *p*+Pb but systematically lower.

High-p_T v_2 is falling to large negative values (see backup) which is from the over-subtraction of nonflow.
This effect is present in *pp* but is larger and sets in at lower p_T in γA (ATLAS-CONF-2020-018)

$v_2(p_T)$ comparison with CGC calc.

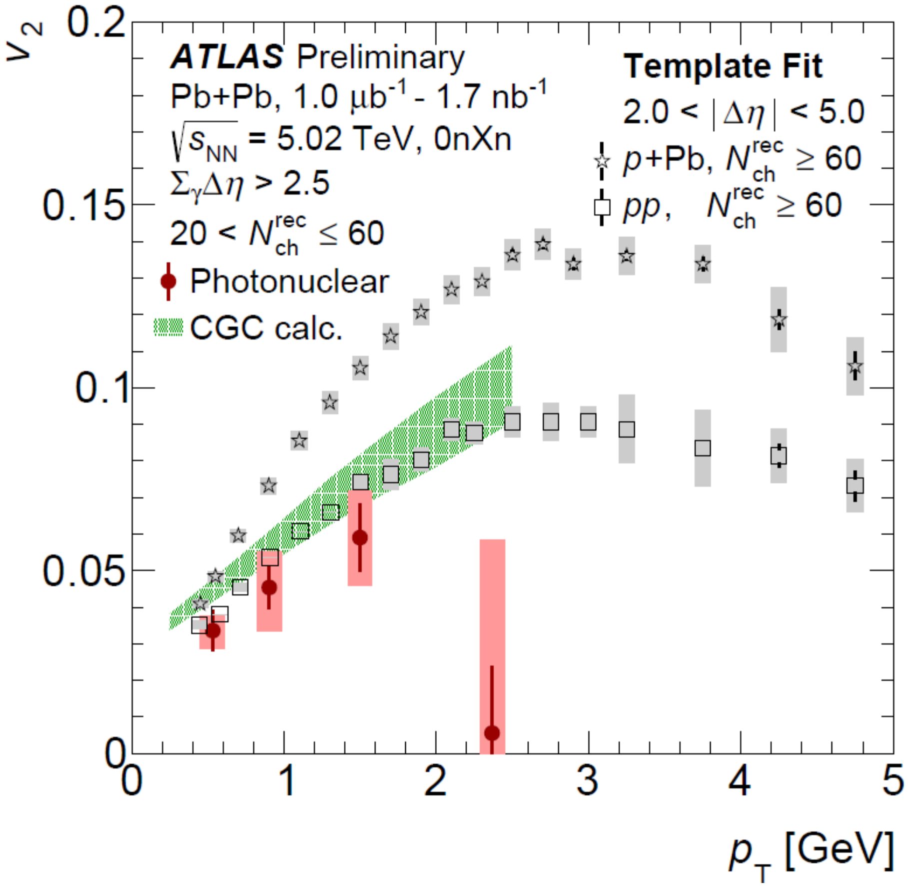

Compared to Color Glass Condensate (CGC) framework calculation of γA $v_2(p_T)$ with Q_s^2 = 5 GeV² and B_P^2 = 25 GeV⁻²

Model is consistent with data at low-p_T

Theory uncertainty from hadron fragmentation

arXiv:2008.03569

CERN-EP-2020-246

CGC model comparison

Color Glass Condensate model calculation containing **initial-state correlations** which gives rise to nonzero v_2

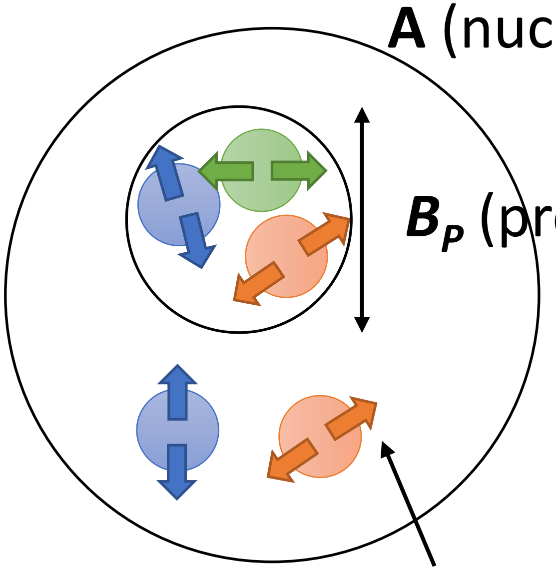

Correlated color domain size is ~ $1/Q_s$

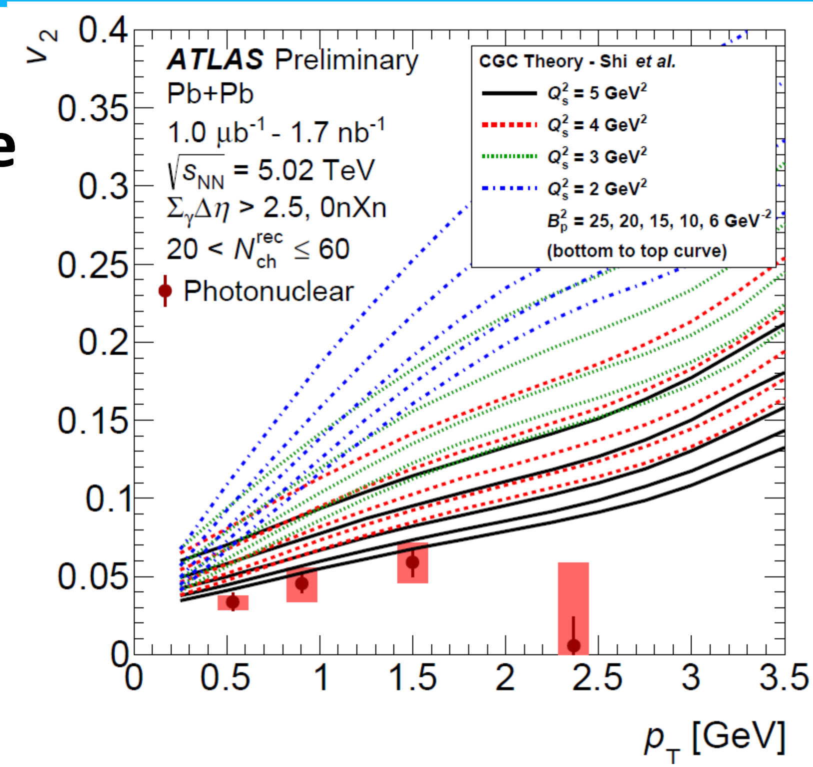

- Larger number of domains struck → lower v_2
- Quasi-real photon is predicted to have large B_P

arXiv:2008.03569

CERN-EP-2020-246

CGC model comparison

Color Glass Condensate model calculation containing **initial-state correlations** which gives rise to nonzero v_2

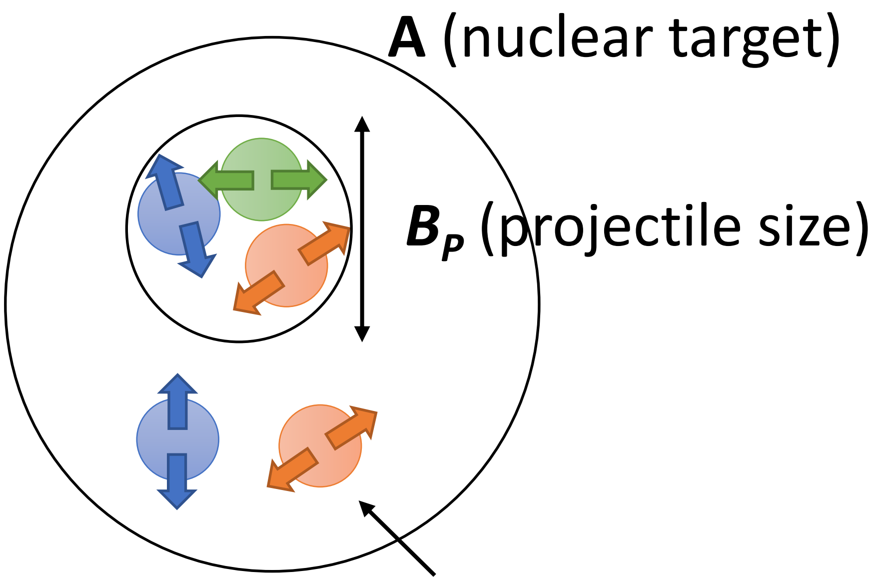

Correlated color domain

size is ~ $1/Q_s$

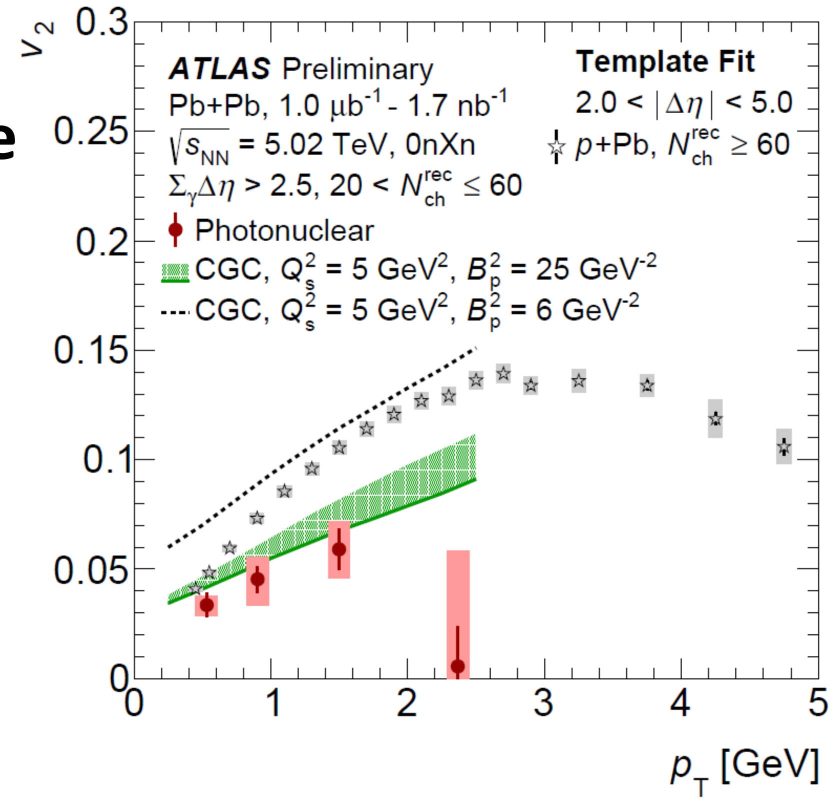

- Similar calculations describing p+Pb (arXiv:1808.09851)
- Difference in v_2 is a result of a smaller B_p^2 for a proton where $B_p^\gamma \sim 1/\Lambda_{QCD}$

CERN-EP-2020-246

Conclusions

Photonuclear v_n has a similar order of magnitude and trends as other previously measured hadronic systems

- Intuitive property of hadronic-like photonuclear collisions (photon $\rightarrow$ vector meson).

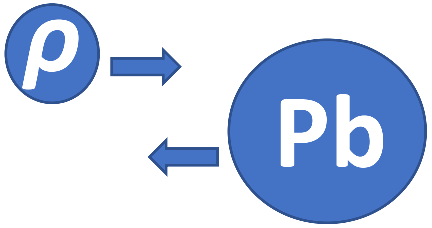

Difference with *pp* might be a consequence of (and further studied by) CM energy, CM-frame rapidity acceptance, and decorrelations effects

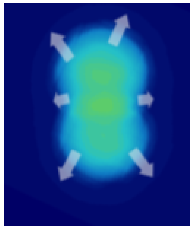

Compared to CGC model and are interested in models which include **final-state effects**.

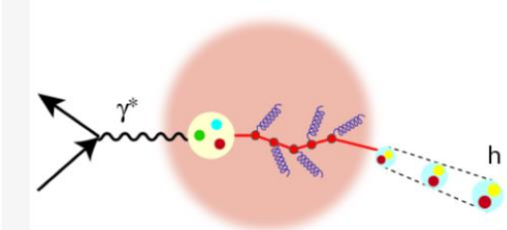

This observation is guiding new theoretical calculations which are relevant for future Electron-Ion Collider data

Universe. 2019; 5(5):98

Thank you

Gap definition (detector roll-out)

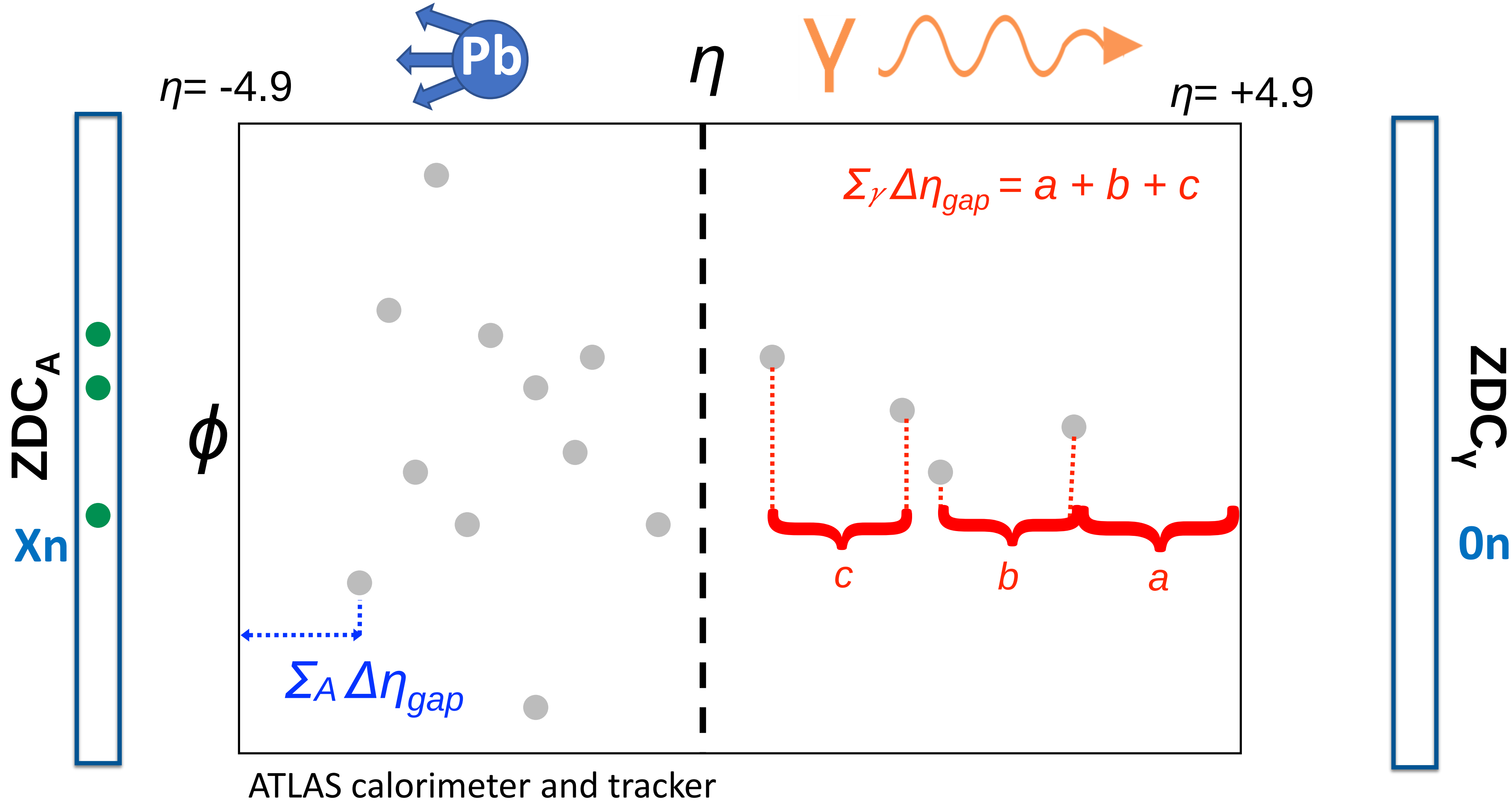

Event Selection: $\Sigma_A \Delta\eta_{gap} < 3$ $\Sigma_{\gamma} \Delta\eta_{gap} > 2.5$

Comparison to DPMJET-III

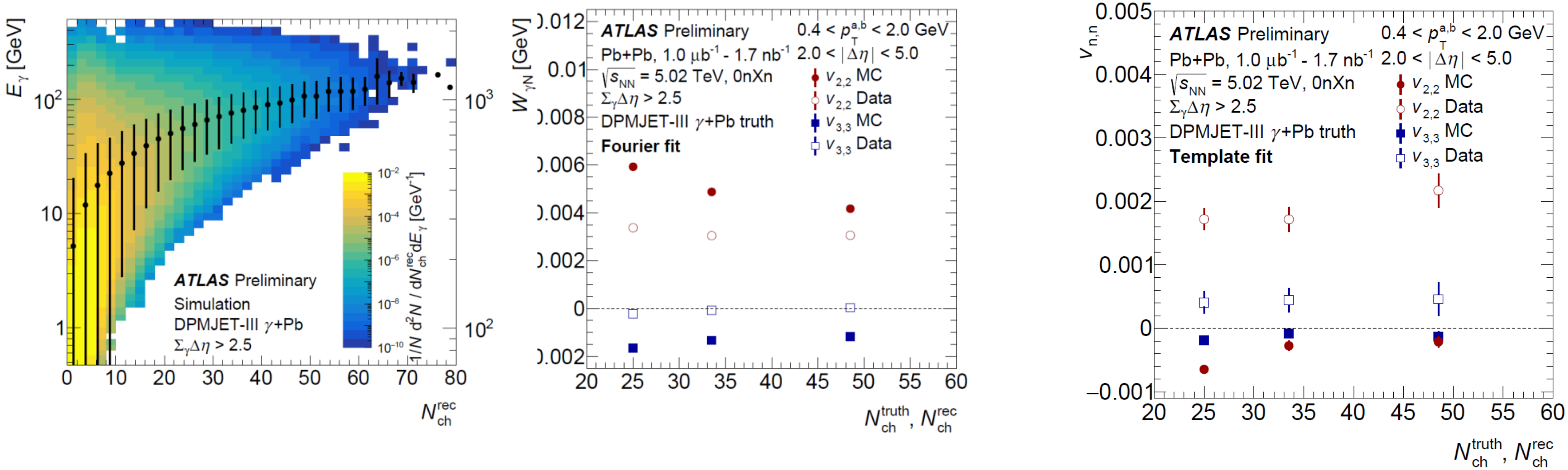

- DPMJET-III predicts the photon energy changes by about 1-2 standard deviations over the multiplicity range of the measurement and a doubling of the mean $W_{\gamma N}$ for 10 to 60 N_{ch}^{rec}.
- Large difference between measured $v_{n,n}$ before and after template nonflow subtraction for data and DPMJET-III.
- Small negative $v_{2,2}$ after template fit

DPMJET-III 2PC example

More jet-like away side in DPMJET-III than in data. This produces the larger unsubtracted $v_{2,2}$ seen on the previous slide. Small remaining modulation after nonflow subtraction seen in the lower panel. DPMJET-III is of limited use in modeling the soft correlations in photonuclear events.

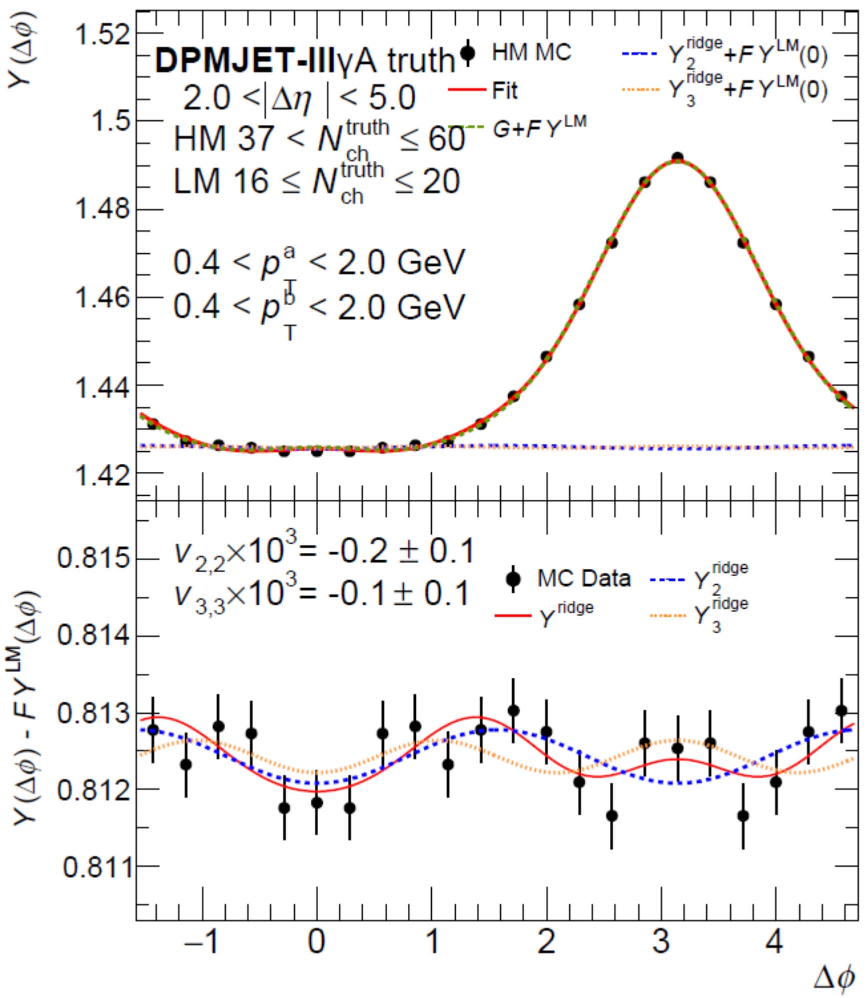

CERN-EP-2020-246

dN_{ch}/dη in γA collisions

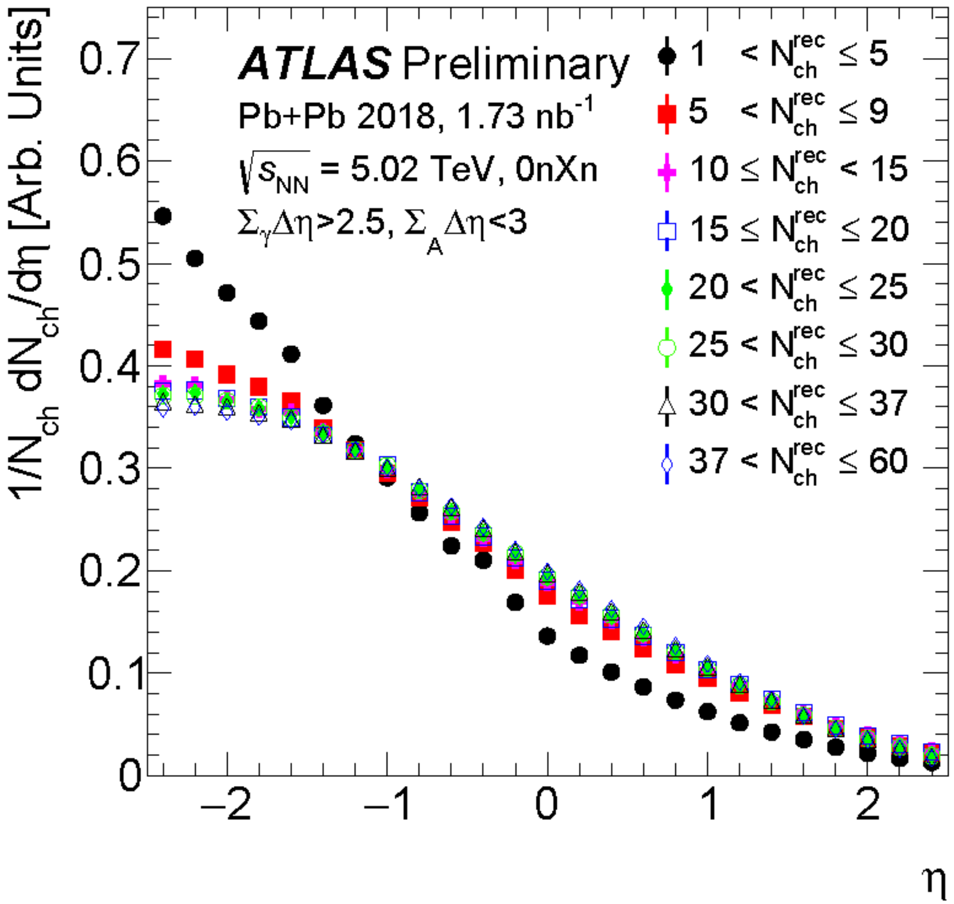

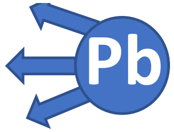

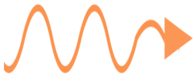

- dN_{ch}/dη of events passing the photonuclear event selection.
- Very similar shape dN_{ch}/dη for events with $N_{ch}^{rec} \geq 10$.

ATLAS-CONF-2019-022

ATLAS template fitting method

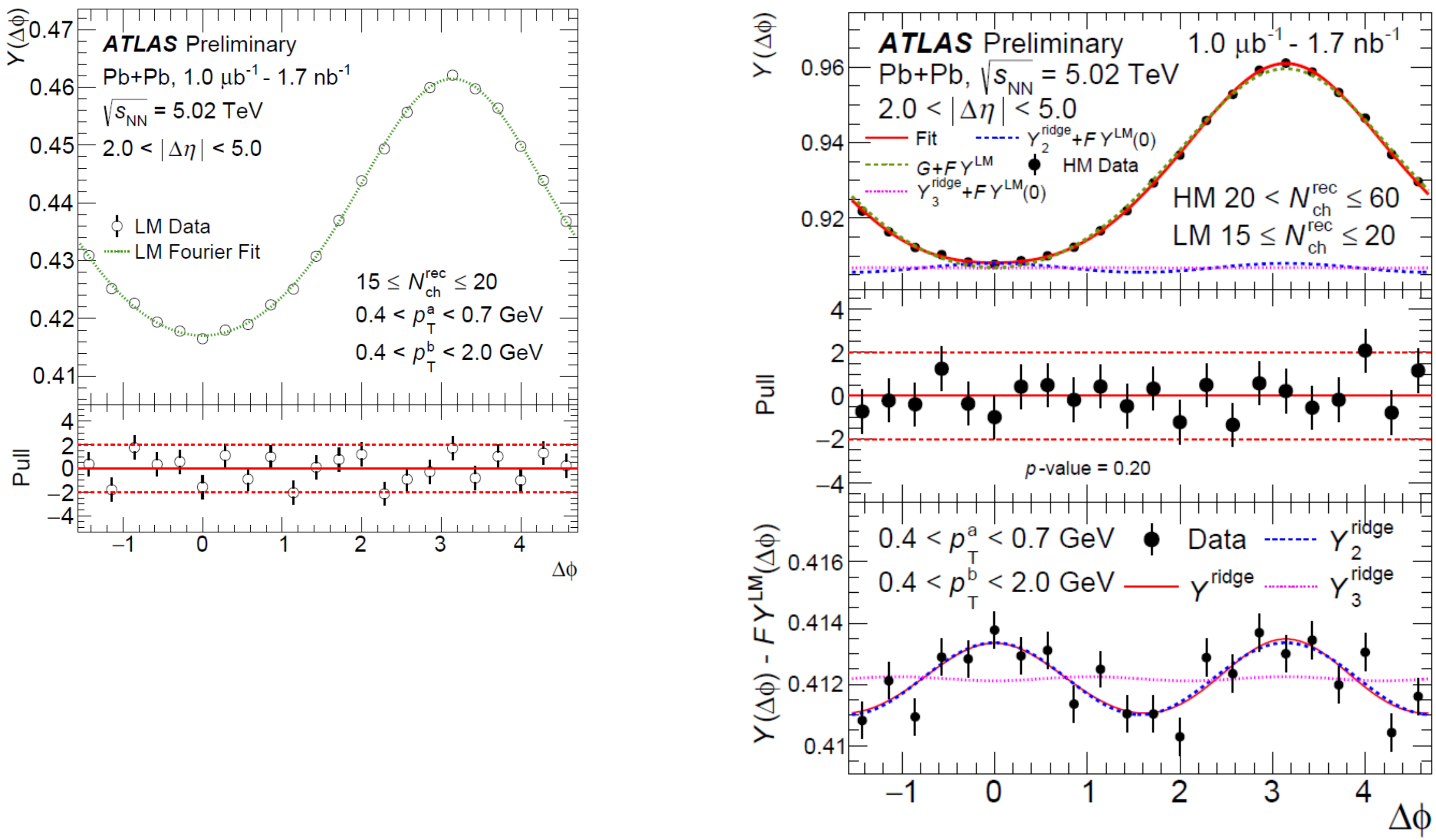

Factorization $v_2(N_{ch})$

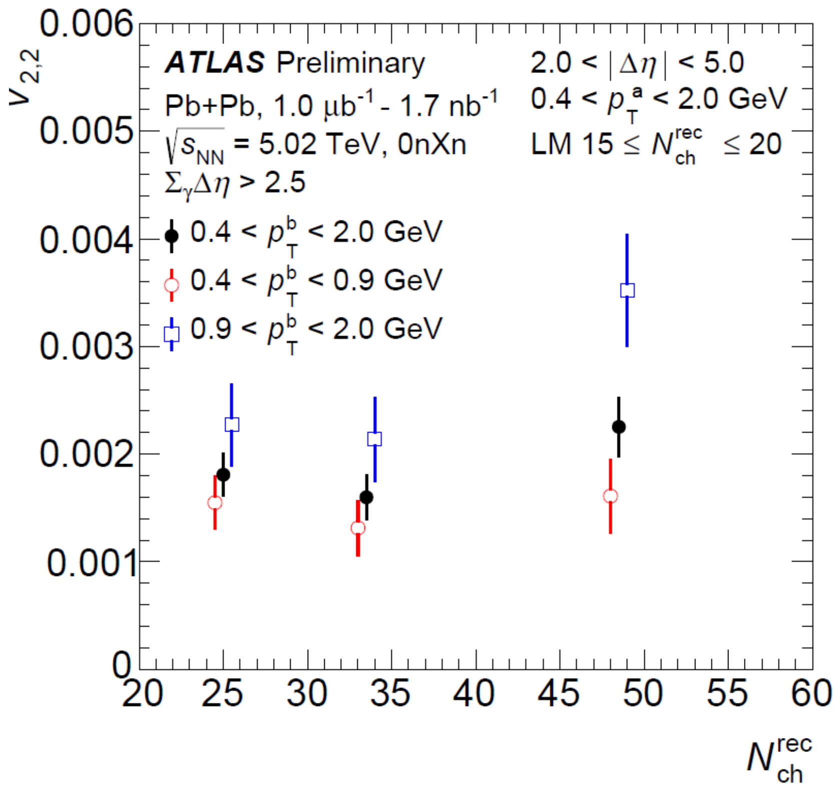

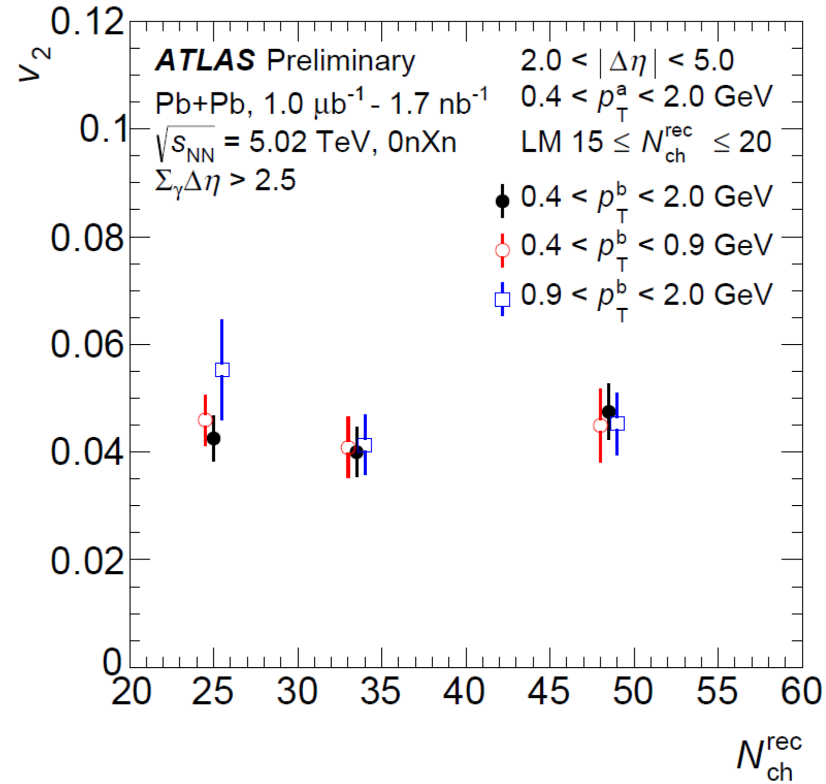

$$v_n(p_T^a) = v_{n,n}(p_T^a, p_T^b)/v_n(p_T^b) = v_{n,n}(p_T^a, p_T^b)/\sqrt{v_{n,n}(p_T^b, p_T^b)}$$

$v_2(N_{ch})$ shows insensitivity to associated particle p_T range. This is consistent with a hydrodynamic paradigm where particle anisotropies are generated from a single-particle flow vector for all p_T.

CERN-EP-2020-246

Photonuclear event properties

Left: N_{ch}^{rec} distribution in data, corrected for trigger and reconstruction efficiency and normalized per event (black points), compared with that in DPMJET-III γ+Pb (dot-dashed green histogram), DPMJET-III γ+*p* (dotted red histogram), and PYTHIA γ+*p* (dashed blue histogram). The bottom panel shows the ratios of the MC distributions to the data distributions. Right: $\Sigma_\gamma \Delta\eta$ distribution in data for $N_{ch}^{rec} \geq 10$ (black points), normalized per event, and compared with that in DPMJET-III γ+Pb (dot-dashed green histogram), PYTHIA γ+*p* (dashed blue histogram), peripheral Hijing Pb+Pb (solid magenta histogram), and DPMJET-III γ+*p* (dotted red histogram).

Right Charged-particle pseudorapidity distribution, $dN_{ch}/d\eta$, in selected N_{ch}^{rec} ranges. The distributions are normalized to the same integral and are shown in arbitrary units. Here, positive and negative η denote the photon-going and nucleus-going directions, respectively. Right: $dN_{ch}/d\eta$ distribution in data for $N_{ch}^{rec} > 10$ (black points), normalized per event, and compared with that in DPMJET-III γ+Pb (dot-dashed green histogram), PYTHIA γ+*p* (dashed blue histogram), peripheral Hijing Pb+Pb (solid magenta histogram), and DPMJET-III γ+*p* (dotted red histogram) with the same reconstruction-level selection as the data. All distributions have been normalized to have the same value as DPMJET-III γ+Pb at η = 0.

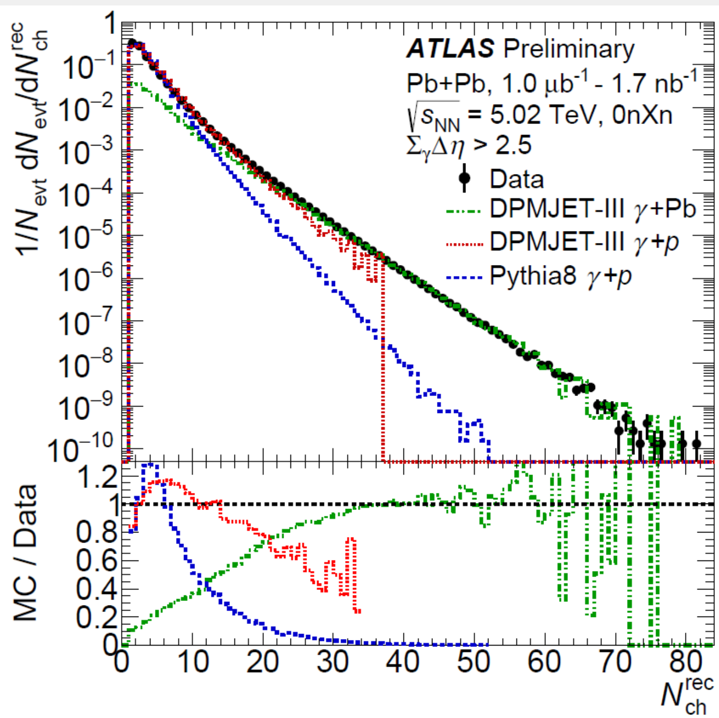

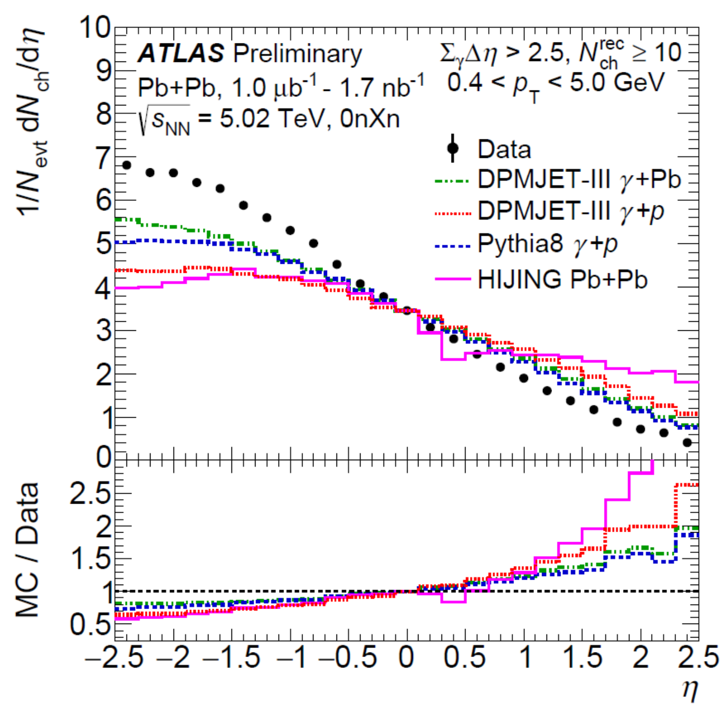

Triggering on photonuclear events

- Due to trigger strategy, the high-statistics portion of the N_{ch} range is for $N_{ch} > 15$

Triggering included

- Level-1 requirements on
  - Minimum event activity to collect high-multiplicity γA events
  - Maximum event activity to reject Pb+Pb collisions
  - Single-sided nuclear breakup (zero-degree calorimeter).
- High-level trigger requirements on
  - Minimum number of tracks to collect high-multiplicity events
  - Maximum energy in photon-going FCAL ($3.2 < \eta < 4.9$)